Improving the Performance of an Operational Flood Early Warning System with the Assimilation of Satellite-Soil-Moisture Data

Santiago Narbondo, Angela Gorgoglione, and Christian Chreties(✉)

Universidad de la República, Julio Herrera y Reissig 565, Montevideo, Uruguay
chreties@fing.edu.uy

Abstract. Soil Moisture (SM) plays a vital role in the hydrologic cycle at watershed scale by influencing the partitioning of precipitation into infiltration, runoff, and evapotranspiration. Therefore, SM assimilation into rainfall-runoff models is considered a way to enhance their performance. Knowing if a storm event is occurring in dry or wet soil conditions means understanding if it may trigger or not a potentially hazardous flood event. Considering the scarcity of *in situ* SM records, satellite SM observations represent a reliable input for improving hydrologic model predictions. In this study, we assess whether the assimilation of satellite SM observations can enhance the water level simulations of an operational early warning system implemented in Uruguay for Durazno city. In particular, the possible improvement is evaluated taking into account the assimilation of SM retrievals from the Advanced SCATterometer (ASCAT). According to the results, an improvement higher than 100% was registered for peak level, and an enhancement higher than 30% was obtained for peak time.

Keywords: Soil Moisture · Flood prediction · Early Warning System · Remote sensing · ASCAT · Uruguay

1 Introduction

Worldwide, river floods represent one of the most frequent and most hazardous natural menaces [1]. Overall, non-structural measures, such as Early Warning Systems and land use planning policies aimed to prevent these catastrophic events, prevail over structural measures, designed, instead, to reduce the consequences of such calamity [1].

Among the non-structural measures, hydrologic and hydrodynamic modeling play a key role. In particular, in hydrologic modeling, a reasonable determination of soil moisture (SM) is essential for a good representation of the hydrologic cycle. SM represents the amount of water that is stored in the pores generated among the unsaturated soil particles. The capability to determine the spatial and temporal distribution of SM is fundamental to explain an integrated system from the hydrologic point of view. In other words, for hydrological, biological, and chemical processes, the knowledge of SM is

© Springer Nature Switzerland AG 2021
O. Gervasi et al. (Eds.): ICCSA 2021, LNCS 12955, pp. 34–46, 2021.
https://doi.org/10.1007/978-3-030-87007-2_3

essential for the exchange of water and energy between the surface and the atmosphere through plant evapotranspiration [2]. Furthermore, SM influences the partitioning of precipitation into infiltration, runoff, and evapotranspiration; therefore, it is a critical factor to define the flood event magnitude [3]. A storm event occurring in dry or wet soil conditions exhibits significant differences in terms of hydrologic response by triggering or not a potentially hazardous flood event [4].

Different techniques for measuring soil moisture can be classified into two main groups: *in situ* (contact-based) and remote sensing (contact-free) [5]. For *in situ* measurements, the main disadvantage is their spatial distribution. In other words, even though they allow accurate measurement of SM near the surface and at different ground depths, they are not capable of representing large-scale spatial distributions [6], e.g., watershed scale. Furthermore, *in situ* measurements are seldom assimilated in hydrologic models due to their scarcity in many parts of the world. For this reason, recently, the number of studies considering coarser SM satellite data is growing tremendously, despite its limitation of surface estimation [7].

Since the 1980s, research results about the estimation of SM from microwave sensors have been published [8,9]. In the last 25 years, the advance of remote sensing with microwaves made it possible to successfully estimate the dielectric properties of the soil surface based on its emissivity and, consequently, estimate humidity [10]. Moreover, in the last 15 years, with the launch of specific missions dedicated to measuring these parameters, the determination of satellite SM has become an increasingly used input in hydrologic modeling. In particular, missions that use low-frequency band sensors (C, X, and L bands) are capable of estimating SM. There are two types of sensors that manage to capture radiation for these uses, active and passive sensors. For the former, the synthetic aperture radars and scatterometers stand out. Among the active sensors, the Advanced Scatterometer (ASCAT) onboard MetOp (Meteorological Operational Satellite) is an instrument that measures the C band operated at a frequency of 5.255 GHz. The central objective of the ASCAT installation is to monitor speed and wind direction over the oceans, and it also has become a good option for SM measurement.

Some experiences have been developed in the assimilation of SM satellite information into hydrologic modeling. For example, in Brocca et al. [11], significant improvements were found when assimilating the daily ASCAT product of 25 km to the "Modello Idrologico SemiDistribuito in continuo" (MISDc) model in the Niccone river basin (140 km^2) in Italy. With the same satellite SM product, in Matgen et al. [12], enhancements in the implementation of the BibModel were found in an experimental basin of 10 km^2 in Luxembourg, where differences in the improvements were determined depending on the season of the year, dividing into dry, humid, and transition periods. Massari et al. [13] used the product of "Satellite Application Facility on Support to Operational Hydrology and Water Management" (H-SAF) derived from ASCAT to apply in five sub-basins of the Tibber River with areas from 140 to 2000 km^2 in Italy, improving flow prediction when assimilating surface and root-zone-SM data in the MISDc model. Patil and Ramsankaran [14] used the ASCAT product to assimilate it to the Soil and Water Assessment Tool (SWAT) hydrologic model in two watersheds of India of 1600 (Wyara river) and 5000 km^2 (Varada river), obtaining moderate improvements in flow simulation.

Uruguay is a country affected by catastrophic flood events that occur with an average frequency of two years. According to the local authorities responsible for emergency management, Durazno is the second-largest city regularly affected by floods, causing significant socio-economic damage [15]. In this context, since 2011, an early warning system (SATI) has been operating to predict extreme events and prevent socio-economical and human-life loss. Although the overall performance of the Durazno warning system is satisfactory, many situations continue to be identified where the rainfall-runoff relationship is not correctly modeled, generating in some cases an underestimation of the peak level up to two meters [16]. This is due to the fact that the humidity condition preceding the event is indirectly represented, based on the precipitation of the five days prior to the event, regardless of the soil type and use in each area of the catchment. This point is highly sensitive in the extreme-event-hydrologic model.

Based on these considerations, the main objective of this study is to assess whether the assimilation of ASCAT SM observations can enhance the water level simulation of the operational early warning system at Durazno city, Uruguay. In particular, the possible improvement will be evaluated taking into account peak level and peak time, the two most critical variables in flood event simulations.

2 Materials and Methods

2.1 Methodology

As shown in Fig. 1, the present work is based on two main blocks. The first block (in green) corresponds to the original SATI operating in Durazno city. It starts with the data acquisition process and continues with the classical hydrological SATI model coupled with the hydrodynamic model. The second block (in red) includes the acquisition of satellite-SM data and the assimilation of such data into the hydrological modeling proposed for the SATI taking into account different formulations. Finally, a comparison of the performance of the different models was carried out.

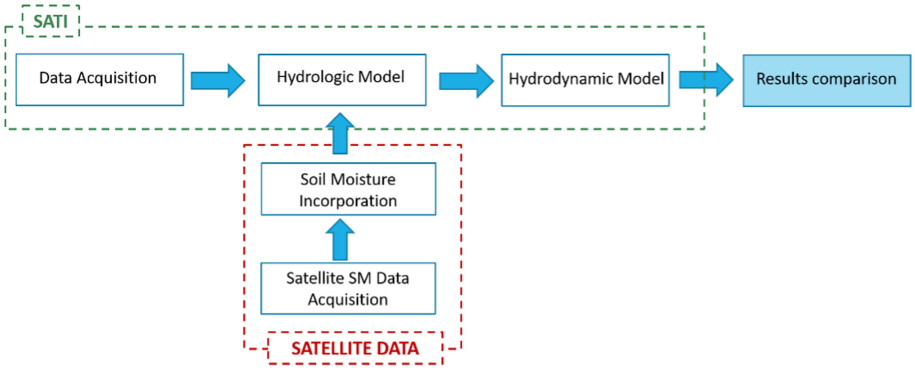


Fig. 1. Flowchart describing the methodological approach (Color figure online).

2.2 Study Area

The area considered in this study is the Yí river basin, located in the central part of Uruguay (South America). Since the city of Durazno is the most affected one by flood events, we focused our study on such a city. Therefore, we considered the Yí watershed with the outlet located at its mouth in the Negro river, including Durazno in the study area (Fig. 2). This watershed has a surface equal to 8,850 km^2 and an average slope of 4.2%. The average available water is equal to 99 mm, and the concentration time is 54 h. The primary land use of the catchment is natural pasture (grassland) used for extensive livestock (82%). Agricultural and forestry land uses also cover a significant surface of the watershed, 9% and 8% respectively.

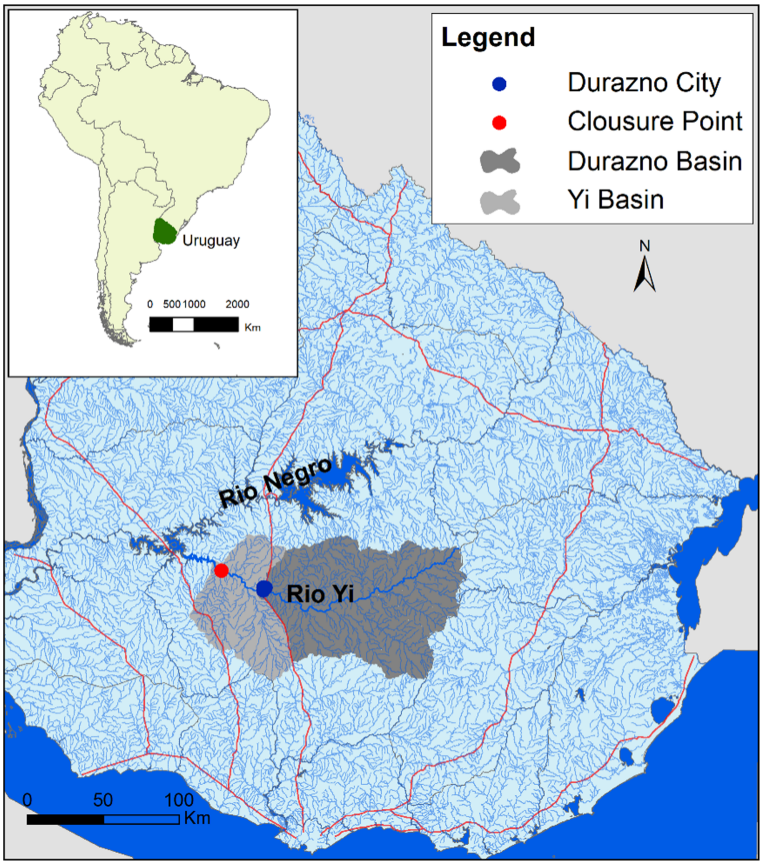


Fig. 2. The Yí river basin and location of Durazno city.

2.3 Data Collection

Satellite Data
For this work, ASCAT SM product was adopted. These observations are available from 2006 to the present. ASCAT uses an active microwave at a frequency of 5.3 GHz (C band) to determine SM content [17]. ASCAT SM provided is related to the SM content of the wettest (field capacity) and driest (wilting point) SM conditions registered [18]. For this product, the cell size is 25 km and estimates the SM for the first 5 cm. It measures the degree of saturation and the values are presented between 0 and 1. The SM is a daily ASCAT product with a few missing values. In particular, for the product used in this work, the level 3 product data were downloaded, provided by National Commission for Space Activities (CONAE) from Argentina, through the viewer of the Satellite Information for Agriculture project (ISAGRO). This information is freely available online and the mission is still operative nowadays. [19].

ASCAT observations were selected for this study for the following reasons: *i)* good performance registered around the world [20] [4] [21]; *ii)* they cover the period where flood events occurred, and water level measurements are available (2013–2020); *iii)* they are available in near-real-time (a few hours after the revisit).

Precipitation and Water-Level Data
Daily precipitation data from four telemetric stations from the National Administration of Power Plants and Transmission (UTE) were used. The mean precipitation series in the basin was obtained according to the Thiessen polygons weighting method.

Water-level data were registered at four hydrometric stations that belong to the Uruguay National Water Board (DINAGUA) and UTE (Fig. 3). The water-level series corresponding to each station has an hourly frequency in 2013–2020, which corresponds to the period in which SM-satellite data are available. Both precipitation and water-level data are freely available online for these stations [22].

Soil Type
The information of the soil type was obtained from the National Commission for the Agro-economic of the Land (CONEAT) soil map, with a scale of 1:40,000, obtained from the General Directorate of Natural Resources of the Ministry of Livestock, Agriculture, and Fisheries (RENARE-MGAP) freely available online [23]. This map provides information about the soil composition based on the percentage of organic matter, silt, sand, and clay [24]. Furthermore, the soil hydrological groups are determined according to the Natural Resources and soil Conservation Service (NRCS) classification with the Soil Recognition map of Uruguay, scale 1:1,000,000 [25] freely available on the web [26].

Flood Events and Soil Moisture Data
The most severe flood events that occurred in the study area were identified, and we selected the ones for which satellite data were available (period 2013–2020) (Table 1). It is worth noting that such events occurred throughout the entire year (during summer and winter), showing the non-stationarity of flood events. This is of particular interest because Uruguay is characterized by high hydro-climatic variability, particularly for precipitation and streamflow [27].

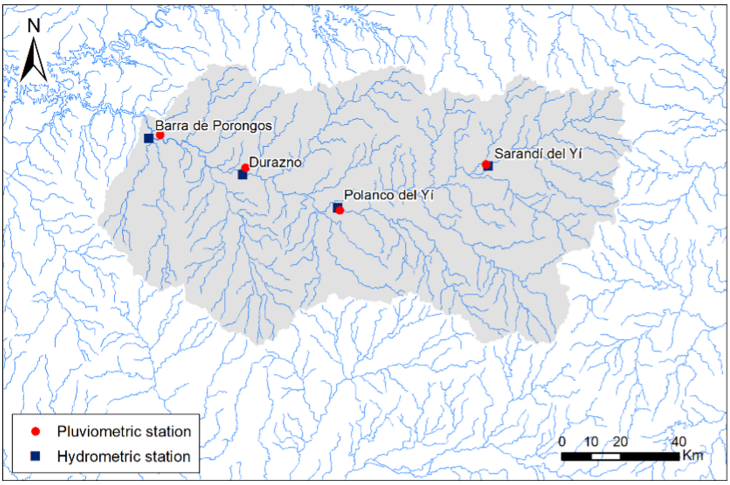


Fig. 3. Telemetric (precipitation) and hydrometric (water level) stations.

Table 1. Selected flood events.

Event name	Start-end (dd/mm/yyyy)	Peak level (m)
Sep-13	09/09/2013–21/09/2013	9.59
Feb-14	25/01/2014–06/02/2014	10.69
Apr-14	05/04/2014–17/04/2014	8.45
Jul-14	27/06/2014–09/07/2014	9.46
Sep-14	18/09/2014–20/09/2014	12.21
Nov-14	01/11/2014–07/11/2014	8.45
Dec-14	22/11/2014–28/11/2014	8.80
Dec-16	20/12/2016–01/01/2016	7.05
Aug-17	25/08/2017–15/09/2017	9.84
Dec-18	18/12/2018–20/12 /2018	8.20
Jan-19	08/01/2019–14/01/2019	11.09
Jun-19	16/06/2019–24/06/2019	12.82
Oct-19	05/10/2019–19/10/2019	10.00
Jun-20	25/06/2014–29/06/2020	9.27

2.4 Rainfall-Runoff and Hydrodynamic Model

For the SATI Durazno, the adopted model consisted of coupling the Curve Number (CN) hydrologic model [28] to the hydrodynamic model implemented in HEC-RAS [29], which solves the flow dynamics equations along the channel and the floodplain in one dimension. The Yi watershed was divided into 16 sub-basins where the hydrologic

model was solved (Fig. 4). The resulting hourly hydrographs were used as input of the hydrodynamic model, while the condition of the downstream edge was the normal tie of the last section of the channel.

The resulting coupled model was successfully calibrated and validated in Silveira et al. [15]. The calibrated parameters were the Manning roughness coefficients in the channel and floodplain, the concentration time, and the CN. In the study of Silveira et al. [15], the calibration of the two models employed an iterative process by varying the parameters mentioned above. Working within the established range and comparing (numerically and statistically) the simulation with the measured water level at Durazno city, the calibration was performed until a good fit was obtained. An in-depth description of the model (SATI) implemented in Durazno, its calibration and validation process and the results obtained are presented in the two works of Silveira et al. [15, 30].

For the system under study, several alert levels are depicted with colors: yellow, orange, and red, respectively ordered from the least to the most dangerous level. Such alert levels are defined based on the infrastructures and households affected by flood events and arise from the analysis of the exposure and vulnerability of the different components of the corresponding spatial system in Durazno city. For this work, the red security alert, corresponding to 8.5 m above the local zero, was considered since it is the most dangerous one. Therefore, improving model predictions related to this alert level would lead to a significant reduction in the number of unnecessary expensive precautions taken by the government (false flood alarms). To this aim, we considered not only events that registered a water level higher than 8.5 m, but also events with water lever close to this threshold to take into account possible false alarms.

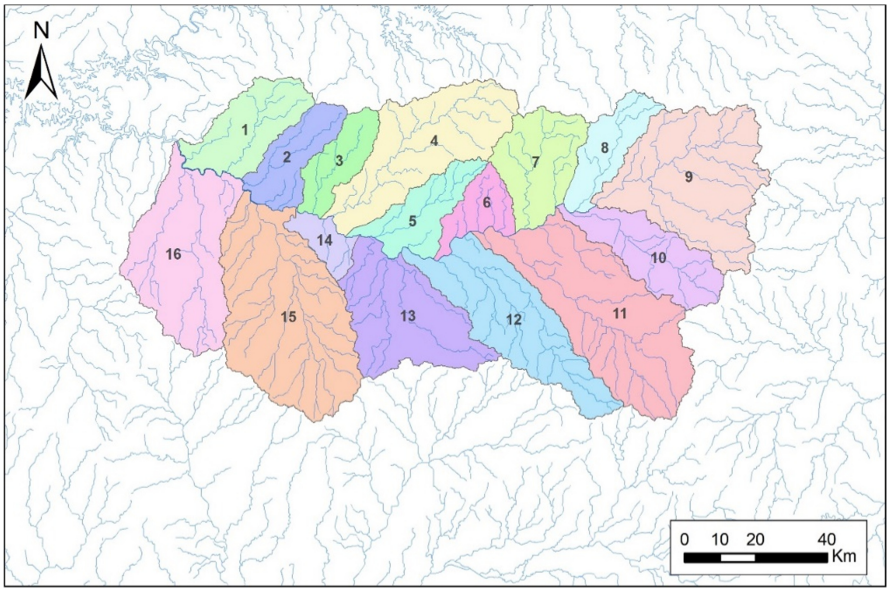


Fig. 4. Sub-basins of the Yí River considered for the coupled hydrologic-hydrodynamic model [30].

From the beginning of SATI Durazno operation, a periodic update of the model performance is carried out for new flood events. This allows us to identify the events where the model showed the best or the worst performance and, therefore, understand the robustness of the SATI Durazno [16].

For the sake of clarification, the expressions "SATI," "SATI Durazno," "current model" refer to the model described in this Section.

Assimilation of Soil Moisture

The assimilation of SM was carried out in the hydrologic model. To this aim, we briefly explain its components related to this process.

The method assumes that the infiltration has two components: one where the infiltration rate is equal to the rainfall intensity, which implies that there is no runoff, and another one where the infiltration rate decreases as a function of time. In this way, the initial abstraction (I_a) and the continued abstraction (F_a) are defined. Thus, the method assumes the relationship between these two variables and precipitation (Eq. 1).

$$\frac{P_e}{S} = \frac{P_e}{P - I_a} \tag{1}$$

P_e represents the effective precipitation [L], and P is the precipitation [L]. Applying the continuity of the event, we have Eq. 2

$$P = P_e + I_a + F_a \tag{2}$$

Defining P_e as Eq. 3.

$$P_e = \frac{(P - I_a)^2}{P - I_a + S} \tag{3}$$

At last, we have Eq. 4 and 5.

$$P_e = 0 \;\rightarrow\; if\; P \leq 0.2S \tag{4}$$

$$P_e = \frac{(P - 0.2S)^2}{P + 0.8S} \;\rightarrow\; if\; P \geq 0.2S \tag{5}$$

Defining S as the maximum storage of the basin [L], knowing that this depends on the use and type of soil and the antecedent humidity conditions. This relationship can be standardized by defining the CN as expressed in Eq. 6

$$S = 25.4\left(\frac{1000}{CN} - 10\right) \tag{6}$$

For the CN model, the possibility of taking the NCII is proposed as an explicit function of the SM content when this measure is obtained. In this way, there is a variable CN that depends on the update of the state of humidity in the basin. This relationship is given by the following formulation (Eq. 7):

$$CN_t = CN(\theta_t) = CN(I) + (CN(III) - CN(I))\left(\frac{\theta_t - \theta_{pwp}}{\theta_{fc} - \theta_{pwp}}\right) \tag{7}$$

θ_t represents the soil water content [L], θ_{pwp} is the wilting point [L], and θ_{fc} is the field capacity [L]. Thus, for each update of the humidity data, the CN is updated, and the effective precipitation is calculated. In this way, there is a CN dependent on humidity and variable according to the antecedent condition. Thus, from the ASCAT SM data, an SM value per sub-basin is calculated for each day of the event and the value of the CN for that day is corrected.

3 Results and Discussion

The results of the 14 events simulated (period 2013–2020) are presented in Fig. 4 and Table 2. In particular, we are showing the comparison between water-level observations and simulations at the red alert levels that corresponds to 8.5 m (red horizontal line in Fig. 5).

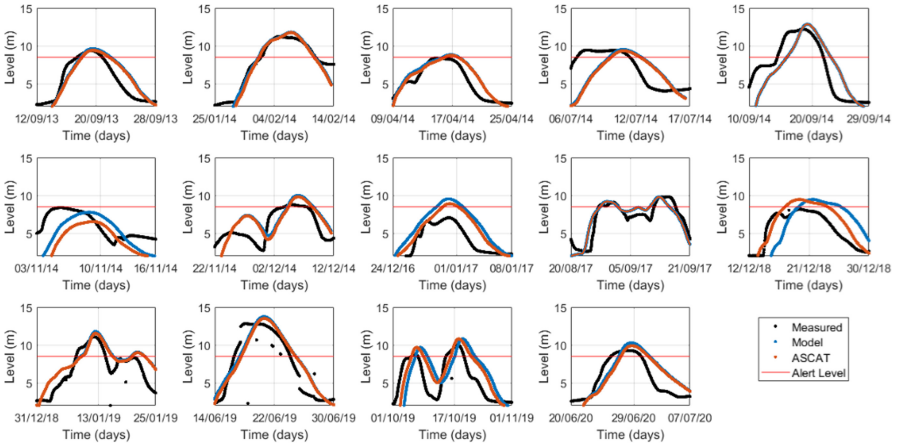


Fig. 5. Comparison between observed (black dots) and simulated limnigraphs obtained with the actual model (SATI) (blue dots) and the actual model + ASCAT (orange dots) for the 14 events (Color figure online).

From the graphs, we can see that the values of the observed peak level are very similar to the simulated ones, with a slight tendency to be closer to the ones obtained with the actual model + ASCAT. If we look at the peak time, the differences between observations and simulations seem to be even smaller. In particular, there is a very similar tendency in their ascending and descending branches, even though the values do not exactly match. This could indicate that although the time and peak level can be improved, the behavior of the measured limnigraph is not fully captured especially in the ascending branch. This can be explained because of the model limitations or by the type of events. On the one hand, the NRCS model indirectly represents the antecedent moisture state, leading to a poor representation of the ascending branch of the hydrograph. On the other hand, the type of event can affect the modeling performance since convective precipitation events can generate more abrupt flood hydrographs that are not correctly captured by

the model. In Table 3 and Table 4, the averaged numerical and statistical results of the peak level and peak time comparison (observed *vs.* actual model and observed *vs.* actual model + ASCAT) respectively are shown. For this comparison, the root mean square error (RMSE), the coefficient of determination (R^2), and the absolute difference between observed and simulated values (AbsDif) were adopted.

Table 2. Values of the peak level and difference of peak time to the peak time measure.

Event name	Peak level			Peak time		
	Observations (m)	Current model (m)	Current model + ASCAT (m)	Observations date (dd/mm/yyyy hh:mm)	Current model (days)	Current model + ASCAT (days)
Sep-13	9.59	9.63	9.39	19/09/2013 03:00	−0.42	−0.46
Feb-14	10.69	11.15	11.06	04/02/2014 18:00	−2.08	−2.08
Apr-14	8.45	8.40	8.22	14/04/2014 21:00	−1.92	−2.00
Jul-14	9.46	9.88	9.70	07/07/2014 12:00	−3.33	−3.38
Sep-14	12.21	13.22	13.22	18/09/2014 15:00	−0.58	−0.58
Nov-14	8.45	8.13	7.66	05/11/2014 12:00	−3.25	−3.63
Dec-14	8.80	10.36	10.17	04/12/2014 18:00	−1.29	−1.29
Dec-16	7.05	8.93	8.14	31/12/2016 02:00	0.04	−0.08
Aug-17	9.84	10.15	10.15	17/09/2017 00:00	−0.50	−0.38
Dec-18	8.20	9.83	9.82	19/12/2018 15:00	−5.00	0.04
Jan-19	11.09	12.13	11.42	12/01/2019 00:00	−0.33	−0.38
Jun-19	12.82	14.10	13.32	18/06/2019 03:00	−2.50	−2.54
Oct-19	10.00	11.16	11.15	17/10/2019 21:00	−0.29	−0.29
Jun-20	9.27	10.63	9.68	28/06/2020 06:00	−0.33	−0.46

Table 3. Averaged numerical comparison between simulated and measured peak levels for the 14-rainfall events.

Model	RMSE (m)	R^2 (–)	AbsDif (m)
Current model	1.11	0.91	0.89
Current model + ASCAT	0.75	0.94	0.62

Table 4. Averaged numerical comparison between simulated and measured peak times for the 14-rainfall events.

Model	RMSE (days)	AbsDif (days)
Current model	2.21	1.56
Current model + ASCAT	1.80	1.26

From the average indicators, we can see a noticeable improvement in the model performance when ASCAT SM is assimilated. In particular, for the peak level, RMSE, R^2, and AbsDif respectively improved by 148%, 97%, and 144%; for peak time, 41% and 31% are the improvements registered for RMSE and AbsDif respectively. This is consistent with the results obtained in Brocca et al. [11], where, for continuous modeling, a value for the Nash-Sutcliffe (NS) efficiency improved from 0.76 to 0.86 due to the assimilation of the SM data in the entire root zone. Also, in Matgen et al. [12], improvements of 15% in the efficiency of the BibModel are obtained. In Massari et al. [13], there are improvements in the MISDc model's efficiency used of up to 30%. Furthermore, in Patil and Ramsankaran [14], the performance of the continuous hydrologic model adopted improved with the incorporation of SM from NS = 0.23 to NS = 0.42 in one of the basins considered in their study, and from NS = 0.25 to NS = 0.70 for the remaining basins of their work. Also, in Chreties et al. [16], certain events were identified in which the difference between the measured water level and the simulated water level was up to two meters. According to this work, this occurred mainly in multimodal events, in part due to the poor representation of the antecedent SM state of the basin simulated by the model. This is partially improved by assimilating the SM data, as can be seen in the August 2017 event, where differences in level and peak time are enhanced. Although some of these errors are corrected, the spatial variability of precipitation should also be explored, as well as the application of continuous models to incorporate SM.

4 Summary and Conclusions

In this study, we demonstrated that the assimilation of ASCAT SM observations substantially improved the water level simulations of the Flood Early Warning Systems currently operating in Durazno city, Uruguay.

To this aim, SM measured with the satellite was assimilated to the hydrologic part of the model. For the flood events between 2013 and 2020, it was found that the difference

in absolute value between simulated and measured is 0.89 m for the current model. According to the results, the current model with the ASCAT data assimilation shows better performance in terms of both peak level and peak time, the two most critical variables in flood event simulations. In particular, an improvement higher than 100% was registered for peak level, and an enhancement higher than 30% was obtained for peak time. In other words, an average improvement of 0.27 m (AbsDif) in terms of peak level is obtained for assimilating ASCAT SM to the current model.

It is clear that the addition of remotely sensed SM to the existing operational Flood Early Warning System increases its accuracy and, therefore, its reliability. Although the amount of satellite data is still a challenge in operational systems, the potential benefit may lead to a substantial reduction of false flood alerts. This will help governments and water managers in reducing the number of unnecessary precautions and increasing the confidence to act upon these flood alerts.

Based on the current promising results, a further step to be considered to improve the model outcomes is the assimilation of other satellite products and other hydrologic models.

References

1. WMO: Manual on Flood Forecasting and Warning. WMO-No. 1072. ISBN 978-92-63-11072-5 (2011)
2. Liang, S., Wang, J.: Advanced Remote Sensing. Academic Press (2019)
3. Koster, R.D., Mahanama, S.P., Livneh, B., Lettenmaier, D.P., Reichle, R.H.: Skill in stream flow forecasts derived from large-scale estimates of soil moisture and snow. Nat. Geosci. **3**, 613–616 (2010)
4. Massari, C., Camici, S., Ciabatta, L., Brocca, L.: Exploiting satellite-based surface soil moisture for flood forecasting in the Mediterranean area: state update versus rainfall correction. Remote Sens. **10**, 292 (2018)
5. Bittelli, M.: Measuring soil water content: a review. HortTechnology **21**(3), 293–300 (2011). https://doi.org/10.21273/HORTTECH.21.3.293
6. Petropoulos, G.P., Griffiths, H., Dorigo, W., Xaver, A., Gruber, A.: Surface soil moisture estimation: significance, controls and conventional. Meas. Tech. (2013). https://doi.org/10.1201/b15610-4
7. Srivastava, P., Kerr, Y.: Satellite Soil Moisture Retrieval: Techniques and Applications (2016)
8. Wang, J., Schmugge, T.: An empirical model for the complex dielectric permittivity of soils as a function of water content. IEEE Trans. Geosci. Remote Sens. **GE-18**(4), 288–295 (1980). https://doi.org/10.1109/TGRS.1980.350304
9. Ulaby, F.T., Moore, M.K., Fung, A.K.: Microwave Remote Sensing, Active and Passive, vol. 3. Artech House, Norwood, MA (1986)
10. Mohanty, B., Cosh, M., Lakshmi, V., Montzka, C.: Soil moisture remote sensing: state-of-the-science. Vadose Zone J. **16**(1), 1–9 (2017). https://doi.org/10.2136/vzj2016.10.0105
11. Brocca, L., Moramarco, T., Melone, F., Wagner, W., Hasenauer, S., Hahn, S.: Assimilation of surface- and root-zone ASCAT soil moisture products into rainfall–runoff modeling. IEEE Trans. Geosci. Remote Sens. **50**(7), 2542–2555 (2012). https://doi.org/10.1109/TGRS.2011.2177468
12. Matgen, P., et al.: Can ASCAT-derived soil wetness indices reduce predictive uncertainty in well-gauged areas? A comparison with in situ observed soil moisture in an assimilation application. Adv. Water Resour. **44**, 49–65 (2012). https://doi.org/10.1016/j.advwatres.2012.03.022

13. Massari, C., Brocca, L., Tarpanelli, A., Moramarco, T.: Data assimilation of satellite soil moisture into rainfall-runoff modelling: a complex recipe? Remote Sens. **7**(9), 11403–11433 (2015). https://doi.org/10.3390/rs70911403
14. Patil, A., Ramsankaran, R.A.A.J.: Improved streamflow simulations by coupling soil moisture analytical relationship in EnKF based hydrological data assimilation framework. Adv. Water Resour. **121**, 173–188 (2018). https://doi.org/10.1016/j.advwatres.2018.08.010
15. Silveira, L., Lopez, G., Chreties, C., Crisci, M.: Steps towards an early warning model for flood forecasting in Durazno city in Uruguay. J. Flood Risk Manag. **5**, 270–280 (2012)
16. Chreties, C., De Vera, A., Crisci, M., Alonso, J., Silveira, L.: Sistema de Alerta Temprana para la previsión de avenidas en la ciudad de Durazno: Evaluación de su desempeño y extensión a otras ciudades de Uruguay. In: Memorias del XXVII Congreso Latinoamericano de Hidráulica, IAHR LAD, Lima, Perú (2016)
17. Wanders, N., Karssenberg, D., de Roo, A., de Jong, S.M., Bierkens, M.F.P.: The suitability of remotely sensed soil moisture for improving operational flood forecasting. Hydrol. Earth Syst. Sci. **18**, 2343–2357 (2014)
18. Wagner, W., Lemoine, G., Rott, H.: A method for estimating soil moisture from ERS scatterometer and soil data. Remote Sens. Environ. **70**, 191–207 (1999)
19. ASCAT Soil Moisture product: Available: http://200.16.81.92/geoexplorer/composer/#Humedad_de_Suelo:_ASCAT_Advanced. Last accessed 10 May 2021
20. Brocca, L., et al.: River flow prediction in data scarce regions: soil moisture integrated satellite rainfall products outperform rain gauge observations in West Africa. Sci. Rep. **10**, 12517 (2020)
21. Cenci, L., et al.: An evaluation of the potential of Sentinel 1 for improving flash flood predictions via soil moisture–data assimilation. Adv. Geosci. **44**, 89–100 (2017). https://doi.org/10.5194/adgeo-44-89-2017
22. Precipitation and water-level data: Available: https://portal.ute.com.uy/precipitaciones-ocurridas-y-prevision-de-niveles. Last accessed 10 May 2021
23. CONEAT soil map: Available: https://www.gub.uy/ministerio-ganaderia-agricultura-pesca/tramites-y-servicios/servicios/consulta-coneat. Last accessed 10 May 2021
24. Molfino, J.H., Califra, A.: Agua Disponible de las Tierras del Uruguay. División de Suelos y Aguas, Ministerio de Ganadería Agricultura y Pesca, Uruguay (2001)
25. MGAP: Carta de Reconocimiento de Suelos del Uruguay, vol. 111. Ministerio de Ganadería, Agricultura y Pesca, Dirección de Suelos y Aguas (1979)
26. Soil recognition map of Uruguay: Available: https://www.gub.uy/ministerio-ganaderia-agricultura-pesca/politicas-y-gestion/carta-reconocimiento-suelos-del-uruguay-escala-110 00000. Last accessed 10 May 2021
27. Narbondo, S., Gorgoglione, A., Crisci, M., Chreties, C.: Enhancing physical similarity approach to predict runoff in ungauged watersheds in sub-tropical regions. Water **12**, 528 (2020). https://doi.org/10.3390/w12020528
28. USDA: Part 630 Hydrology -National Engineering Handbook (NEH). Natural Resources Conservation Service, U.S. Department of Agriculture, Washington, DC (2010)
29. US Army Corps of Engineers: HEC-RAS 4.1 Hydraulics Manual. US Army, Washington (2011)
30. Silveira, L., Chreties, C., Crisci, M., Usera, G., Alonso, A.: Sistema de Alerta Temprana Para Previsión de Avenidas En La Ciudad de Durazno. Innotec (10), 56–63. https://doi.org/10.26461/innotec.v0i10 (2015)